Scripta Materialia 196 (2021) 113765

Contents lists available at ScienceDirect

Scripta Materialia

journal homepage: www.elsevier.com/locate/scriptamat

# Suppression of abnormal grain growth in friction-stir welded Al–Cu–Mg alloy by lowering of welding temperature

Ivan S. Zuiko[a,*], Sergey Mironov[a], Sergey Betsofen[b], Rustam Kaibyshev[a]

[a] Laboratory of Mechanical Properties of Nanoscale Materials and Superalloys, Belgorod National Research University, Pobeda 85, Belgorod 308015, Russia
[b] Moscow Aviation Institute, National Research University, Moscow 109383, Russia

ARTICLE INFO

*Article history:*
Received 12 October 2020
Revised 25 January 2021
Accepted 26 January 2021
Available online 6 February 2021

*Keywords:*
Aluminium alloys
Friction-stir welding
Abnormal grain growth
Electron backscatter diffraction (EBSD)
Transmission electron microscopy

ABSTRACT

The effect of welding temperature on thermal stability of friction-stir welded (FSWed) 2519 aluminum alloy was investigated. A lowering of the welding temperature below the particle dissolution threshold was shown to be a very effective way for suppression of abnormal grain growth during post-weld solution treatment. This effect was attributed to a prevention of the welded material from precipitation of fine dispersoids during subsequent annealing which resulted in relatively low Zener pressure and thus provided an activation of the apparently-normal grain-growth mechanism. This phenomenon was demonstrated for the first time and could be used as a processing strategy to improve thermal stability of FSWed heat-treatable alloys.



Friction-stir welding (FSW) is an advanced solid-state joining technique that has significant industrial potential [1]. Unfortunately, an essential drawback of this technology is a relatively low stability of the welded materials against abnormal grain growth [e.g. 2–11]. This undesirable phenomenon involves catastrophic growth of a few grains, which consume almost entire weld zone and thus considerably degrade weld performance.

It is important to emphasize that thermal stability of friction-stir welded materials is essentially sensitive to FSW conditions. Specifically, a lowering of welding temperature usually decreases the grain-growth onset temperature [2–10]. In *non-heat treatable* aluminum alloys, this effect is usually attributed to a formation of relatively fine-grained structure and the concomitant increase of the total grain boundary energy. In this context, it is worth noting, that the final grain size in fully-annealed low-temperature welds is typically of several hundred microns only, thus being comparatively small. This effect arises from a relatively competitive character of the grain growth. In contrast, high-temperature welds with relatively coarse-grained structure are stable until higher annealing temperatures but the subsequent grain growth has a pronounced abnormal nature, and the final grain size achieves a mm-scale [e.g. 3,4].

Annealing behaviour of *heat-treatable* aluminum alloys is additionally affected by second-phase particles, thus being more complicated. The abnormal grain growth in friction-stir welds of such materials is usually attributed to the dissolution of constituent second-phase particles in the stir zone [e.g. 2,3,5] and is typically explained in terms of the Humphreys' cellular theory [12]. In the authors' recent work, however, it has been shown that a lowering of FSW temperature may efficiently suppress the precipitation dissolution [13]. In this regard, it has been suggested that the particle retention may improve the thermal stability of welds. The present study was undertaken in order to examine a reliability this idea.

The program material used in this work was a commercial 2519 aluminum alloy (a nominal chemical composition of Al–5.64Cu–0.33Mn–0.23Mg–0.15Zr–0.11Ti–0.09V–0.08Fe–0.08Zn–0.04Sn–0.01Si; all in weight %). This is a typical heat-treatable alloy whose FSW- and ageing behaviours are studied relatively well [14–16]. The material was produced by ingot casting, homogenized at 510°C for 24 hours, and then rolled to a true strain of 0.88 at 425°C. To obtain a precipitation-hardened condition, the hot-rolled material was T820 tempered, i.e., solutionized at 535°C for 1 hour, water quenched, cold-rolled to a true thickness reduction of 0.22, and then artificially aged at 165°C for 6 hours. 3-mm-thick sheets of the tempered material were friction-stir welded by using a commercial AccurStir 1004 FSW machine. The welding tool consisted of a concave-shaped shoulder with a diameter of 12.5 mm and an M5 cylindrical probe with a length of 2.7 mm. To investigate an effect of the welding temperature, several different FSW regimes were selected, as shown in Table 1. It was found, however, that annealing behaviour of high-temperature welds was broadly similar to each other. For sake of simplicity, therefore, only

* Corresponding author.
*E-mail address:* zuiko_ivan@bsu.edu.ru (I.S. Zuiko).

https://doi.org/10.1016/j.scriptamat.2021.113765
1359-6462/

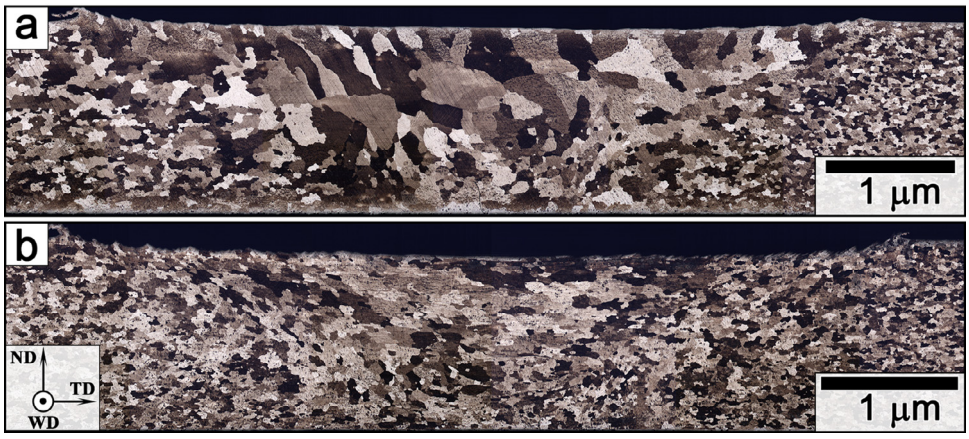


**Fig. 1.** Optical macrographs showing effect of FSW temperature on subsequent annealing behaviour of friction stir welded material: high-temperature weld (a) and low-temperature weld (b). The reference frame for both welds is shown in the bottom left corner of (b); WD, ND and TD are welding direction, normal direction, and transverse direction, respectively. In all cases, advancing side is left and retreating side is right. Note suppression of abnormal grain growth in the low-temperature weld.

**Table 1**
FSW conditions employed in the present work.

| Welding condition | Spindle rate, rpm | Feed rate, mm/min |
|---|---|---|
| Low-temperature | 500 | 760 |
| High-temperature | 500 | 125 |
| | 1100 | 380 |
| | 1100 | 125 |

Note: The high-temperature weld considered in the present study is highlighted with gray.

a single high-temperature weld produced at a spindle rate of 1100 rpm and a feed rate of 380 mm/min was studied in the present work. On the other hand, it was also established that a decreasing of FSW temperature below the low-temperature condition studied resulted in welding defects.

To examine thermal stability of the produced welds, those were solutionized at 535°C for 1 hour followed by water quenching. Microstructural observations were conducted using optical microscopy, electron backscatter diffraction (EBSD), transmission electron microscopy (TEM), and x-ray diffraction (XRD) technique. For optical observations, the specimens were prepared by mechanical polishing in conventional fashion followed by chemical etching in a Keller's reagent and the subsequent immersion in 0.5% water solution of HF. The grain-size distributions derived from optical micrographs were based on ~500 measurements for each material condition. The final surfaces for EBSD- and TEM-analyses were obtained by electro-polishing in a 25% solution of $HNO_3$ in $CH_3OH$. EBSD maps were acquired using an FEI Nova NanoSEM 450 field-emission-gun scanning electron microscope equipped with a TSL OIM™ EBSD system and operated at an accelerated voltage of 30 kV. In all cases, the obtained EBSD maps consisted of ~10,000 grains. A 15° criterion was used to differentiate low-angle boundaries (LABs) from high-angle boundaries (HABs). For TEM examinations, a JEM-2100 transmission-electron microscope operated at 200 kV was employed. The size-distributions and volume fractions of second-phase particles were quantified on a basis of ~500 measurements for each studied material condition. XRD analysis was performed using a Rigaku SmartLab diffractometer equipped with Cu K$\alpha$ radiation source. The specimens were scanned over the angular range of 30 to 145º at a rate of 0.01º/min.

Low-magnification optical macrographs of the welds subjected to the final solutionizing treatment are shown in Fig. 1* and supplementary Fig. S1. As expected, high-temperature welds experienced abnormal grain growth (Fig. 1a and supplementary Fig. S1). On the other hand, low-temperature joint showed a relatively uniform microstructure distribution and no clear evidence of the catastrophic grain growth was found (Fig. 1b). These observations were in excellent agreement with the basic idea of this work, i.e., a simple lowering of FSW temperature below the particle dissolution threshold was effective for suppression of the abnormal grain growth.

In order to check a reliability of this result, it was treated in terms of the Humphreys' cellular model [12]. According to this theory, the grain-growth mechanism (i.e. either normal or abnormal) of a particle-containing material is governed by a relationship between mean grain size $R$, particle volume fraction $F_v$, and the mean particle size $d$, and is expressed by a dimensionless parameter $Z = \frac{3F_vR}{d}$. Therefore, to evaluate the thermal stability of both the high- and low-temperature welds, the above microstructural characteristics were quantified in as-welded material conditions by using EBSD and TEM techniques. The obtained results were summarized in Figs. 2, 3, and Table 2.

As expected, FSW resulted in fine-grained recrystallized microstructures in the stir zones of both welds (EBSD maps in Fig. 2). Remarkably, HABs fraction in both welds constituted ~70% of the total grain boundary area. To the first approximation, therefore, both materials could be considered as *ideal grain assemblies*, in which all grain-boundary energies and mobilities are equal, i.e., the Humphreys' model is applicable for microstructural analysis. Importantly, both material conditions contained evenly distributed second-phase particles (TEM micrographs in Fig. 2), i.e., those were not completely dissolved during high-temperature welding†.

The low-temperature weld was characterized by a finer grain size, coarser particle size, and higher particle volume fraction than the high-temperature weld (Fig. 3 and Table 2). All these effects were presumably associated with relatively low welding temperature which inhibited grain boundary migration and particle dissolution during FSW. In terms of the $Z$-value, however, the revealed difference was relatively small (Table 2). Importantly, the abnormal grain growth was predicted to occur in both welded conditions according to the Humphreys' theory (Table 2).

The latter result was very confusing. It required a fundamental reconsideration of the grain growth behaviour.

* Grain size distributions for the low- and high-temperature welds are given in supplementary Fig. S2a.

† X-ray measurements revealed a prevalence of $\theta$ phase among the second-phase particles (supplementary Fig. S3). However, TEM-EDS examinations also showed a presence of $\beta'$ and T phases (supplementary Fig. S4).

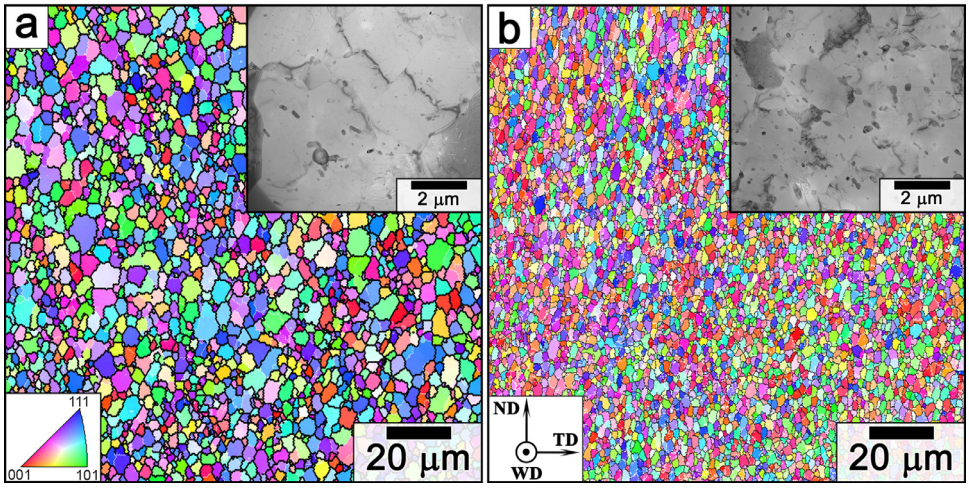


**Fig. 2.** Selected portions of EBSD maps and TEM images showing typical microstructures evolved in the stir zone of high-temperature weld (a), and low-temperature weld (b) in as-welded condition (the TEM micrographs are shown as inserts in the top right corners). In EBSD maps, individual grains are colored according to their crystallographic orientation relative to welding direction, and LABs and HABs are depicted as white and black lines, respectively.

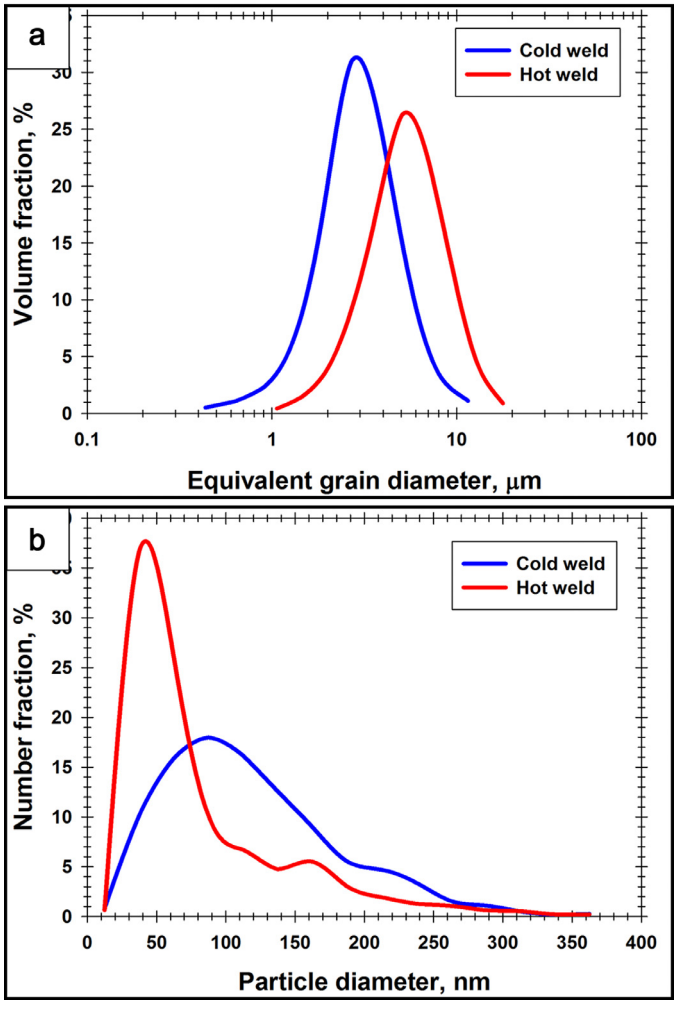


**Fig. 3.** Grain-size distributions (a) and particle-size distributions (b) as function of welding conditions. Note: The data were measured in as-welded conditions. The grain-size data were derived from EBSD maps whereas the particle statistics was measured from TEM data.

The primary issue was the role played by the second-phase particles during microstructural coarsening. As the solutionizing treatment (employed in the present study) implies the complete dissolution of the particles, they perhaps could not exert any influence on the grain growth process. On the other hand, it is known that the gross grain-boundary migration in fine-grained aluminum alloys initiates above ~250°C [17]. Therefore, there was a possibility that the welded material may experience significant microstructural changes during *heating stage* of the solutionizing annealing. To examine this idea, an additional set of the welded specimens were heated to the solutionizing temperature (~ 5 minutes) and then immediately water quenched. The produced microstructures are shown in Fig. 4‡. It is seen that the microstructures of both welds experienced significant coarsening. In the high-temperature weld (Fig. 4a), this process was obviously governed by the abnormal mechanism, whereas the low-temperature weld (Fig. 4b) exhibited an apparently normal grain growth. Therefore, it is clear that the extensive grain growth occurred below the precipitation dissolution temperature, and thus the mechanism of the microstructural coarsening process was influenced by the secondary particles.

As the program material used in the present work was a *heat-treatable alloy*, it may experience significant changes in terms of particle volume fraction and size during heating. Therefore, the particle characteristics measured at ambient temperature (Fig. 3b and Table 2) presumably altered before the annealing temperature exceeded the grain-growth threshold (i.e., ~250°C). The possible changes expected in the low- and high-temperature welds are discussed below.

As shown in the authors' previous work [13], FSW temperature in *low-temperature welds* is not sufficient for the particle dissolution and thus no supersaturated solid solution develops. Accordingly, the subsequent heating of such welds up to the grain-growth temperature could not result in precipitation phenomena and thus the particle volume fraction remains unchanged. Accordingly, the particle evolution should be dominated by their coarsening. This reduces the particle Zener pressure, lowers the *Z*-value, and thereby shifts the grain growth behaviour towards the activation of the normal mechanism.

On the other hand, the extensive particle dissolution is usually reported for *high-temperature FSW* [1,3,13]. Consistently, pro-

‡ Appropriate grain size distributions are given in supplementary Fig. S2b

**Table 2**
Microstructural characteristics of welded material and predicted annealing behaviour.

| Material condition | Mean grain size R, $\mu$m | Volume fraction of particles $F_v$ | Mean particle size d, nm | Z value | Expected annealing behaviour |
|---|---|---|---|---|---|
| Low-temperature weld | 1.8 | 0.019 | 119 | 0.86 | Abnormal grain growth |
| High-temperature weld | 3.5 | 0.008 | 86 | 0.98 | Abnormal grain growth |

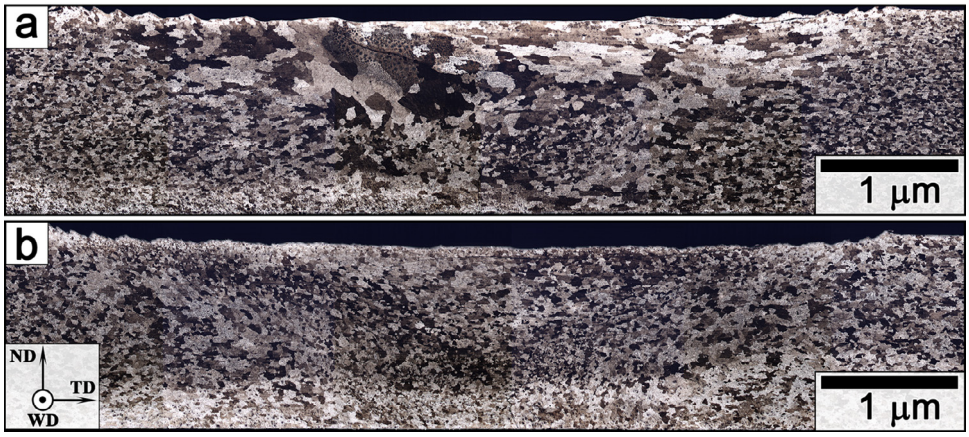


**Fig. 4.** Optical macrographs showing microstructural changes occurred during heating stage of solutionizing treatment: high-temperature weld (a) and low-temperature weld (b). Note: Both welded specimens were immediately quenched after achieving of solutionizing temperature of 530°C. The reference frame for both welds is shown in the bottom left corner of (b); WD, ND and TD are welding direction, normal direction, and transverse direction, respectively. In all cases, advancing side is left and retreating side is right.

nounced precipitation phenomena are expected during subsequent annealing and therefore the particle volume fraction should increase. Considering the relatively low temperatures and very short duration of the precipitation process, the size of the freshly-nucleated particles should be small and thus the average particle diameter should decrease. All these changes should enhance the particle Zener force, increase the Z-value, and thus promote the abnormal grain growth.

Despite the above theory is in a good agreement with the real annealing behaviour (Figs. 1 and 4) and seems to be reasonable, it is important to emphasize that it is entirely speculative and thus warrants further experimental verification.

In conclusion, a lowering of FSW temperature below the particle dissolution threshold was shown to be an effective way for the suppression of abnormal grain growth during post-weld treatment. This result was attributed to distinctly different particle behaviour. In high-temperature welds, the secondary particles dissolve during FSW, and thereby the subsequent annealing resulted in re-precipitation of fine dispersoids. This provided a relatively high Zener pressure and thus gave rise to the abnormal grain growth. In low-temperature welds, the precipitates retained in the material, and therefore the post-weld treatment resulted only in particle coarsening. This lowered the particle Zener force and thus promoted activation of the apparently-normal grain-growth mechanism.

## Declaration of Competing Interest

The authors declare that they have no known competing financial interests or personal relationships that could have appeared to influence the work reported in this paper.

## Acknowledgment

The authors are grateful to the personnel of the Joint Research Center “Technology and Materials” at Belgorod National Research University and Dr. S. Malopheyev for experimental assistance.

## Supplementary materials

Supplementary material associated with this article can be found, in the online version, at doi:10.1016/j.scriptamat.2021.113765.

## References

[1] R.S. Mishra, Z.Y. Ma, Mater. Sci. Eng. R 50 (2005) 1–78.
[2] I. Charit, R.S. Mishra, Scr. Mater. 58 (2008) 367–371.
[3] Kh.A.A. Hassan, A.F. Norman, D.A. Price, P.B. Prangnell, Acta Mater. 51 (2003) 1923–1936.
[4] Y.S. Sato, H. Watanabe, H. Kokawa, Sci. Tech. Weld. Join. 12 (2007) 318–323.
[5] M.M. Attallah, H.G. Salem, Mater. Sci. Eng. A 391 (2005) 51–59.
[6] M.A. Safarkhanian, M. Goodarzi, S.M.A. Boutorabi, J. Mater. Sci. 44 (2009) 5452–5458.
[7] H.J. Liu, X.L. Feng, Mater. Des. 47 (2013) 101–105.
[8] Y. Chen, H. Ding, J. Li, Z. Cai, J. Zhao, W. Yang, Mater. Sci. Eng. A 650 (2016) 281–289.
[9] K. Chen, W. Gan, K. Okamoto, C. Kwansoo, R.H. Wagoner, Metal. Mater. Trans. A 42 (2011) 488–507.
[10] E. Cerri, P. Leo, J. Mater. Proc. Technol. 213 (2013) 75–83.
[11] Q. Pang, J.H. Zhang, M.J. Huq, Z.L. Hu, Mater. Sci. Eng. A 765 (2019) 138303.
[12] F.J. Humphreys, Acta Mater. 45 (1997) 5031–5039.
[13] A. Kalinenko, K. Kim, I. Vysotskiy, I. Zuiko, S. Malopheyev, S. Mironov, R. Kaibyshev, Mater. Sci. Eng. A 793 (2020) 139858.
[14] I. Zuiko, R. Kaibyshev, J. Alloy Compd. 759 (2018) 108–119.
[15] I. Zuiko, R. Kaibyshev, Mater. Sci. Eng. A 737 (2018) 401–415.
[16] I.S. Zuiko, R. Kaibyshev, Mater. Sci. Eng. A 793 (2020) 139148.
[17] P.B. Prangnell, J.R. Bowen, P.J. Apps, Mater. Sci. Eng. A 375-377 (2004) 178–185.